Microelectronic Engineering 239-240 (2021) 111526

Contents lists available at ScienceDirect

Microelectronic Engineering

journal homepage: www.elsevier.com/locate/mee

Research paper

Nanolitography based on electrospun and etched nanofibers

Aileen Noori [a], Hilal Döğer [b], Yasemin Demirhan [a], Mehtap Ozdemir [a,c], Lutfi Ozyuzer [a], Gulnur Aygun [a], Özge Sağlam [d,*]

[a] Department of Physics, Izmir Institute of Technology, Urla, 35430 Izmir, Turkey
[b] Division of Bioengineering, Graduate School, Izmir University of Economics, Sakarya Cad. 156, Balcova, 35330 Izmir, Turkey
[c] Teknoma Technological Materials Inc., Izmir Technology Development Zone, Urla, 35430 Izmir, Turkey
[d] Faculty of Engineering, Izmir University of Economics, Sakarya Cad. 156, Balcova, 35330 Izmir, Turkey

ARTICLE INFO

Keywords:
Nanofibers
Nanolithography
Nanofabrication
Direct writing
Electrohydrodynamic method

ABSTRACT

In this study, we propose a new type of nanolithography procedure to fabricate orderly patterned metallic nanostructures using the electrohydrodynamic method and the reactive ion etching process. The electrohydrodynamic process parameters were tuned so as to create patterning with precision, and fibers in nanoscale on silver-coated substrates. We also studied reactive ion etching with different durations on the well-patterned samples. The experiments show that applying a voltage of 400 V resulted in straight patterned fibers with a diameter of 208.7 ± 30.3 nm. The statistical analysis on scanning electron microscope (SEM) images showed a significant difference in the diameter of the fibers fabricated at 400 V compared to those at 500 V and 600 V. We also confirm that the etching process has no affect on the fiber diameter. Moreover, electron dispersive X-Ray spectrometer (EDX) results suggest that an etching duration of 7 min is sufficient to remove the silver coating that is not covered with the fibers, and protect the silver nanostructures underneath the fibers. Utilizing a low-cost nanolithography procedure, we obtain the orderly patterned silver nanostructures for possible integration into miniaturized devices.

1. Introduction

Electrohydrodynamic direct-writing printing, a versatile technique for fabrication of nano−/microfibers, has been widely used in various applications, such as flexible energy storage devices [1–3], flexible electronics [4–7], tissue engineering [8–10], field-effect transistors [11–13], and lab-on-a-chip devices [14–16]. This technique combines electrospinning and three-dimensional printing to construct low-cost, high-resolution, precisely controllable, and fibrous structured patterns or geometries. Optimally positioning and tuning the fibers' diameter is a crucial task in applying the electrohydrodynamic direct-writing printing method. Specifically, the gap between the needle and the collector, the applied voltage, the nozzle/needle structure, the collector's speed, and the pump flow rate are the main factors affecting the fiber morphology and orientation [17]. It is important to keep the distance between the electrode and the collector less than 1 cm to ensure continuous fibers with diameters of less than 100 nm when the applied voltage is relatively low [18]. Moreover, the viscosity, concentration, molecular weight, conductivity, and surface tension of the polymer (the main content of the ink), also play a critical role in printing precisely controlled nanofibers [19].

The electrohydrodynamic technique allows fabrication and alignment of conducting and flexible electrodes in the nanometer-scale. More recently, there have been numerous studies investigating the implementation of the electrospun electrodes into electronic devices. Lee et al. have reported large-scale patterning of polycrystalline copper nanowire arrays with an average nanofiber diameter of 710 nm with 14.1 μΩ cm resistivity after a two-step calcination process [20]. They also demonstrated that the silver nanowire arrays can be fabricated by replacing copper content with the silver trifluoroacetate to produce a nanofiber diameter around 695 nm with an excellent thermal stability after a single step annealing process [21]. Another study demonstrated the electrospinning of kilometers-long, highly conductive silver fibers with the minimum diameter of ~200 nm for flexible electronics [22]. Orderly aligned patterns can also be produced for the usage in wire bonding into the integrated circuits by embedding nanowires or nanoparticles in the polymer matrix. The printed ribbons containing silver nanowires and polyethylene oxide composite structures were created by optimizing

* Corresponding author.
E-mail address: ozge.saglam@ieu.edu.tr (Ö. Sağlam).

https://doi.org/10.1016/j.mee.2021.111526
Received 3 November 2020; Received in revised form 29 January 2021;
Available online 13 February 2021

polymer and process parameters [23]. Moreover, polymers, including nanoparticles, were utilized to produce aligned, conductive, and transparent electrodes with a minimum diameter of 500 nm at high applied voltage [24]. The results of above-mentioned studies imply that electrospinning of the polymers with a conductive nature can cause flashovers, limiting the control of the precise nanopatterning due to the discharge of the high applied voltage between the needle and the collector [25]. Another patterning method with precision in nanotechnology is electron-beam lithography using focused beams of electrons and photoresists [26]. However, this technique is both expensive and challenging to use on large scale applications and requires a high vacuum environment.

In this study, we focused on developing a new low-cost lithography procedure using electrospun nanofibers fabricated by the electrohydrodynamic method. Unlike the studies mentioned above, we used nanofibers as a tool, instead of simply relying on their conductive nature. The direct patterning of polyethylene oxide was performed to allow the nanofibers to form a mask for the protection of the metal parts underneath the fibers. Thus, firstly, electrospun nanofibers were placed on silver-coated substrates by direct writing. In order to reach the optimal conditions (i.e. ideal physical properties and patterning of the fibers), we studied the process parameters of applied voltage, the tip-to-collector distance, platform speed, feed rate of the polymer, and type of auxiliary electrode. The metal surface, covered with nanofibers, was etched by ion beam etching to attain the patterned metallic nanostructures. An EDX analysis of elemental distribution showed that nanofibers were successful in protecting metal regions. To examine the thickness and three-dimensional morphology of the nanofibers before and after the etching process, we used atomic force microscopy (AFM) to confirm that that the fibers were not etched, and that the silver underneath fibers was still intact. These results suggest that it is possible to successfully develop a new lithography procedure to obtain metallic nanoarchitectures without the need for advanced facilities and optical masks.

2. Materials and methods

The polyethylene oxide (PEO) in powder was purchased from Sigma Aldrich (average Mv ~4,000,000) and used as received. The PEO solution at 2 wt % was prepared in deionized water by stirring for 96 h and left to rest for 30 h at room temperature. The precise patterning can be obtained at low voltage without fibers breaking using a stretchable polymer with long polymeric chains [27]. Therefore, we selected a superelastic polymer with a high molecular weight for a continuous electrospinning process.

A single syringe pump was used to supply the solution to a flat-ended stainless steel 30-gauge needle from a 1 mL syringe. The tip-collector surface distance was adjusted to approximately 1 mm to apply near-field electrospinning for a precise printing. A homemade substrate stage controlled by computer software was moved in the x-y axis. To achieve the optimized conditions for the patterning, we used two different techniques for initiating Taylor cone. In the first, an auxiliary electrode was mounted for 1 mm underneath the substrate and aligned with the upper needle, as illustrated in Fig. 1 (a). The voltage was applied at 1 kV between the top needle and the bottom electrode. The flow rate was kept constant as 2.5 μL/h, and Si/SiO_2 substrates were patterned. In the second technique, a low level of voltage between 0.4 and 0.6 kV was applied between the needle and the substrate, as shown in Fig. 1 (b). Silver coated Si/SiO_2 substrates were placed on the movable stage. The polymer was supplied to the needle at a rate of 1 μL/h.

In general, the polymer jet cannot overcome the surface tension between the droplet and air because of voltage difference [27]. Therefore, a tungsten microprobe was applied manually to start the nanofiber fabrication, overcoming the surface tension by initiating a high local electrical field.

The zero-shear viscosity of the polymer was measured by a rheometer (TA Instruments Discovery HR-2). The surface morphology and elemental composition of the fibers were examined by SEM (FEI Quanta 250 FEG) combined with the EDX (Oxford Aztec). The nanofiber thickness and diameter were examined by tapping-mode AFM (Hitachi AFM5100N).

Approximately 100 nm thick silver was coated on Si/SiO_2 substrates by a physical vapor deposition system (Leybold Univex 300) operated at a rate of 0.7 Å/s under $\sim 10^{-6}$ Torr. The etching of the samples was performed by argon ion beam etching system (a custom-made set-up) with a rough pump, a turbomolecular pump (Agilent Varian Turbo-V 301), an etching chamber, a multi-gas controller (MKS Instruments Type 647C), an end-Hall type ion source (Advanced Energy MCIS-12), a DC power supply (Advanced Energy Pinnacle Plus), a close cycle cooling system, a thermocouple vacuum gauge, and a cold cathode gauge controller [28]. The base pressure of the chamber was below 3×10^{-6} Torr, and the pressure during etching was $\sim 10^{-3}$ Torr. The plasma etching conditions were 30 sccm Ar, 70 mA beam current, 750 V beam voltage, and 49 W DC power.

The angle between the incident ion beam and the substrate surface was kept at 22.5° during the etching process because directing the beam perpendicularly at the sample can easily cause damage due to high etching and heating rates. The tilting of the holder provides greater control over the sidewalls of the sample and greater axial stability, and also prevents the possibility of redeposition of etched atoms onto the ion gun surface [29]. Therefore, the sample holder was also rotated with the rotary feedthrough for a smoother etched surface.

We also performed a lift-off process to remove the polymer on the silver patterns. A methanol-water mixture with a 2:1 ratio was gently poured onto the substrate, which was then placed into the mixture at 50 °C for 14 min.

Data collected from SEM images were statistically analyzed with one-way ANOVA, where grouping factors were “applied voltage” and “etching process”. After a group effect from one-way ANOVA, *P*-values of the post hoc *t*-test were presented in P(A, B) format. The A and B

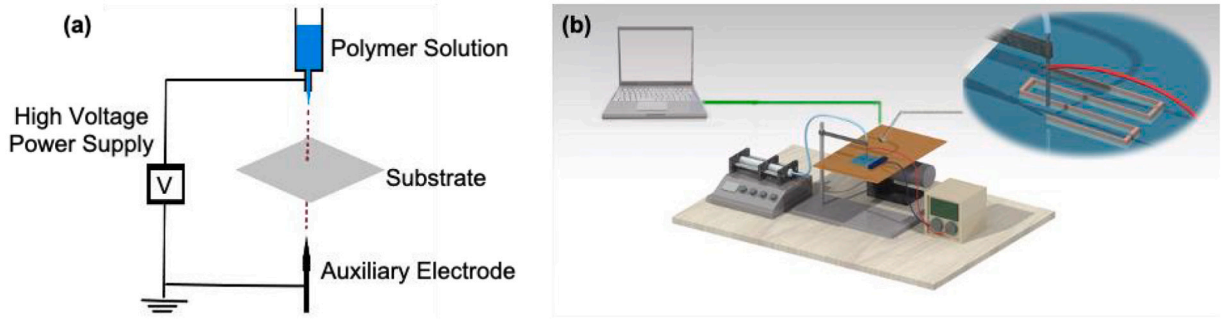

Fig. 1. (a) The schematic showing how the electric field was applied between the needle and the auxiliary electrode (b) the experimental setup of the electrohydrodynamic method, including the x-y stage controlled by a computer software, a power supply and a syringe pump.

represent the groups that were compared with respect to different parameters e.g., applied voltage (400 V, 500 V, 600 V), and the etching process (as-deposited, 5 min, 7 min). SEM images of the 7 min etched samples were also analyzed due to the line edge roughness by a Matlab® based image processing software [30].

3. Results and discussion

The zero-shear viscosity of the 2% PEO solution was determined as 28.48 Pa·s. This value is in agreement with previous findings (e.g., 28.70 Pa·s reported in [27]) and is a suitable value for patterning of the fibers via electrospinning. The slight difference is due to variations in the preparation procedure of the polymer. In general, platform speed and the applied voltage are two critical factors affecting the structure and printing of the nanofibers [31]. Therefore, the first method using an auxiliary electrode was studied with the platform speed of 95 or 250 mm/min to achieve straight fibers in the nanoscale range. Fig. 2 shows the optical micrographs of the fibers patterned with 95 mm/min. The schematic of the pattern designed to be fabricated is illustrated in Fig. 2 (c). The lower platform speed resulted in spiraling of the fibers with the smallest width, approximately 0.35 μm. Although continuous and almost completely straight fibers were produced, as shown in Fig. 2(b), the edgy corners could not be printed as proposed (Fig. 2 (a)). Fig. 3 displays the results of patterning of the fibers at a higher platform speed. Even though the spiraling fiber geometry was not observed, it was not possible to print the pattern due to the platform's high-speed, as demonstrated in Fig. 2 (c) and therefore a simpler grid pattern was printed as shown in Fig. 3 (a, b). Consequently, to the best of our knowledge, this is the first report of nanofibers' patterning with a needle-type electrode as an auxiliary electrode, which was placed underneath the substrate and parallel to the nozzle.

The conventional far-field electrospinning is studied with a distance of 5–15 cm and an applied voltage of 10–20 kV [19]. On the other hand, maintaining a distance of between 500 μm – 5 cm is approved as near-field mode of the electrospinning, essential for the accurate patterning of fibers and achieving a stable jet [32]. Both methods investigated in the current study can be considered as near-field electrospinning. However, the applied voltage could not support a stable jet that would allow precise printing because the second needle was mounted underneath the substrate. The second technique, i.e. patterning with the grounded substrate rather than using an auxiliary electrode, allows the system to operate at lower applied voltage, resulting in thinner fibers. Applying the electric field directly onto the collector created a highly concentrated electric field [33] that was accompanied with lowering the flow rate of the polymer to 1 μL/h. After conducting a series of experiments, 700 mm/min was identified as optimized platform speed to operate at lower applied voltage. The platform speed should be retained higher than the first procedure because of the intensive electric field created by grounding the substrate. To investigate the effect of voltage on the fiber diameter, three samples coated with silver were applied at 400 V, 500 V, 600 V and printed in a straight-line pattern. Fig. 4 displays the samples' SEM images prepared with an increasing applied voltage from top to bottom. Similar to the conventional electrospinning process, it is also possible to control the diameter of nanofibers by changing the voltage. Thinner fibers with a diameter in the range of 208.7 ± 30.3 nm were achieved by decreasing the voltage to 400 V.

Far-field electrospinning fabricates fibers with larger diameters when a higher voltage is applied because a greater amount of polymer is ejected [34]. On the other hand, near-field electrospinning favors the production of thicker fibers at higher voltage due to the reduction of bending instabilities [18]. Bisht et al. reported that it was possible to control nanofibers' morphology, and their diameter and patterning on 2D and 3D substrates using the appropriate PEO ink formulation [27]. The study proposed a continuous, direct writing with a low voltage of 200 V with relatively slower collector speeds of 20–40 mm/s. On the other hand, when the patterns were fabricated at 600 V, instead of straight fibers, looped fibers were observed due to the bending instabilities. We also used the same concentration of the polymer with a different preparation method. Moreover, other studies have demonstrated that nanofibers at higher applied voltages with a faster stage speed could be directly written [35,36]. Huang et al. presented a high voltage near-field direct writing with 800 V applied voltage and 400 mm/s collector speed and fabricated straight patterns with approximately 200 nm thick fibers [35]. In another study, nanofiber diameter was reduced to ~40 nm when 120 mm/s collector speed was applied with the voltage of 500 V [36]. Therefore, in this study we selected a voltage between 400 and 600 V for the fabrication of nanofibers for a straight morphology.

Our objective was not only to achieve straight fibers with nanoscale diameters but also to demonstrate the methodology of a new type of lithography technique. In this regard, the samples were etched after performing the electrohydrodynamic method by ion beam etching to remove the silver coating that was not covered by nanofibers. Fig. 4. also displays SEM images of patterned nanofibers before and after etching with different durations. As shown in SEM results, the diameter varied along the length of a fiber, as also observed in previous reports [36,37]. Therefore, the fiber diameter data measurements from SEM images were analyzed to elucidate the effect of the voltage and etching process on the fiber morphology.

The effects of a larger diameter with the voltage were statistically tested with one-way ANOVA, suggesting that at least one group is different from the others (One-way ANOVA, $F(2, 46) = 42.2$, $p < 0.001$, for "as-deposited"). Post hoc *t*-test for pairwise comparison shows that changing applied voltage from 400 V to 500 V or 600 V significantly increased the diameter ($P(400\ V, 500\ V) < 0.05$, $P(400\ V, 600\ V) < 0.05$), and the diameter did not further increase after 500 V. The analysis was also carried out to check whether the similar effect of applied voltage was observed on the etched fiber diameters. The analysis confirmed that at least one voltage group (i.e. 400 V, 500 V, 600 V) was different from the others (One-way ANOVA, $F(2, 43) = 142.3$, $p < 0.001$,

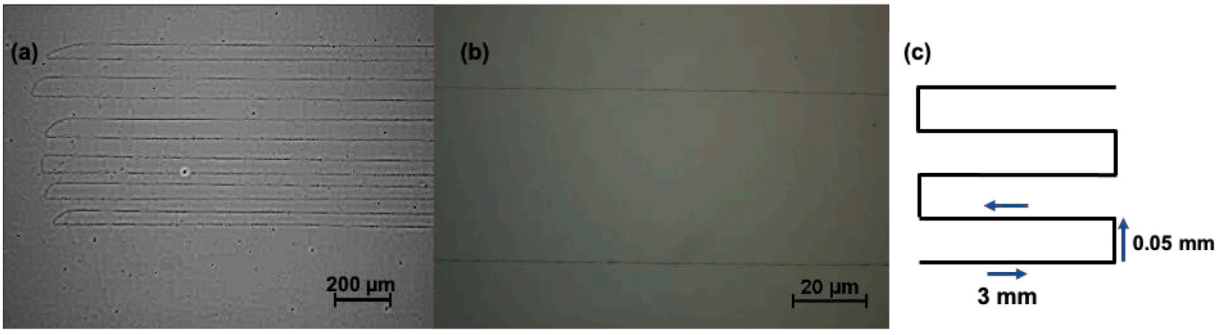

Fig. 2. Optical micrographs of the patterns fabricated with an auxiliary electrode at the deposition speed of 95 mm/min (a) 10× magnification (b) 100× magnification (c) the schematic illustration of the pattern.

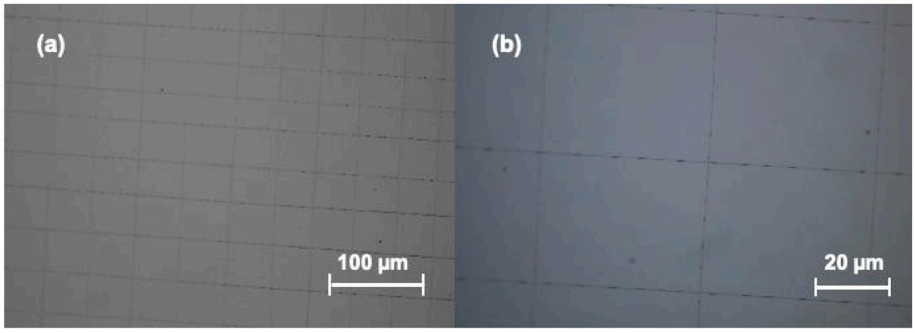

Fig. 3. Optical micrographs of the patterns fabricated with an auxiliary electrode at the deposition speed of 250 mm/min (a) 20× magnimagnification (b) 100× magnification.

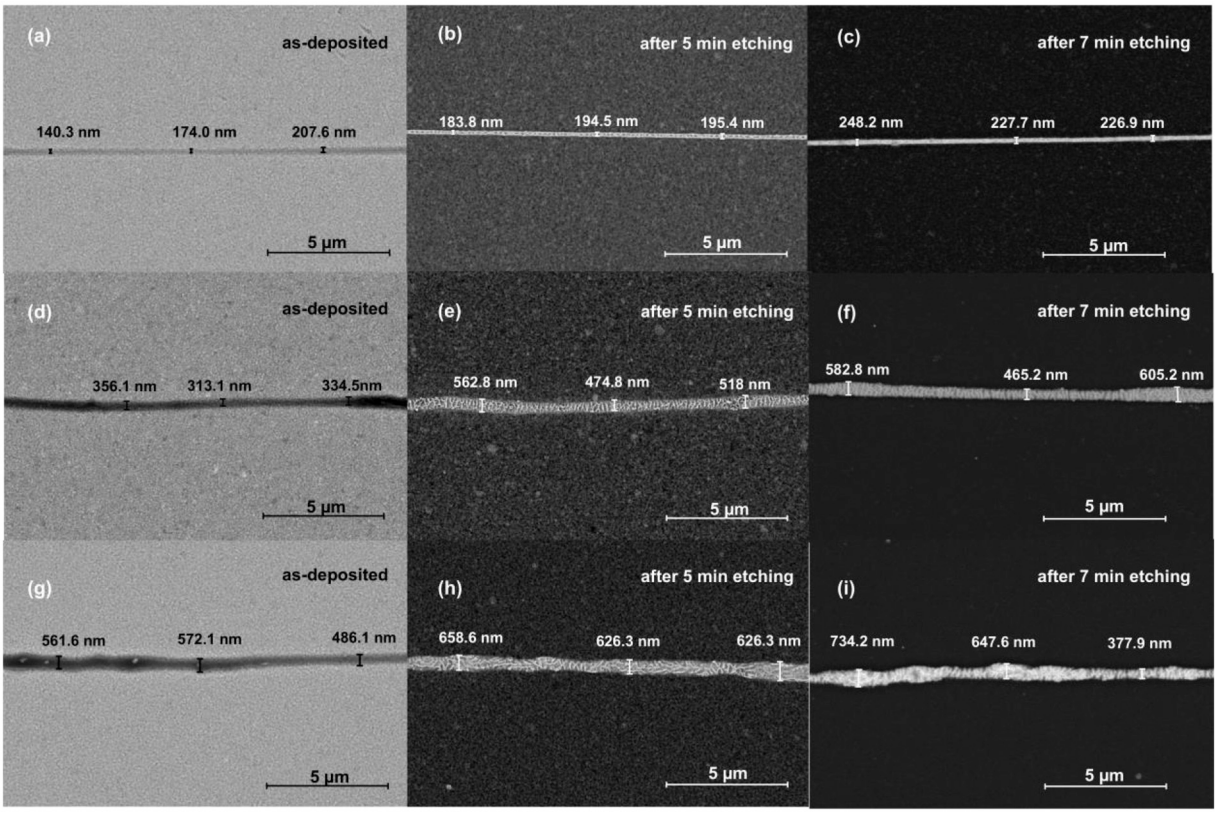

Fig. 4. SEM images of the samples fabricated by the second technique and patterned at an applied voltage of (a–c) 400 V, (d–f) 500 V, and (g–i) 600 V.

for "5 min"; $F(2, 42) = 45.3$, $p < 0.001$, for "7 min"). Post hoc t-test for pairwise comparison for etched samples suggests that with increase in the voltage [$P(400\ V, 500\ V) < 0.05$, $P(400\ V, 600\ V) < 0.05$, for "5 min" and "7 min") there was no increase in the fiber diameter after 500 V [$P(500\ V, 600\ V) = 0.14$, for "5 min"; $P(500\ V, 600\ V) = 0.39$, for "7 min"]. Analysis of the effect of the etching process on the fiber diameter fabricated at different voltages showed no significant differences between etching groups (i.e. "as-deposited", "5 min", "7 min"; One-way ANOVA, $F(2, 51) = 0.7$, $p = 0.5$ for 400 V; $F(2, 35) = 2.29$, $p = 0.12$ for 500 V; $F(2, 48) = 1.54$, $p = 0.22$ for 600 V). The results confirmed that fiber diameter did not change with the etching process, or the duration of the etching process up to 7 min, which was a critical point in time for the nanolithography technique. Moreover, the mean value of LER of the 7 min etched sample fabricated at 400 V was calculated as 22.58 ± 3.57 nm (inspection length: 2 µm) by measuring 15 different spots in SEM images.

To confirm the removal of silver coating on the uncovered parts, and the presence of the silver underneath the nanofibers, we performed an EDX analysis on the fibers and uncovered spots of the sample etched for 5 and 7 min (see Fig. 5). In the case of 5 min of etching, it was still possible to observe the silver coating was on the uncovered parts and underneath the nanofibers, and etching was applied for a further 2 min to remove the silver from the exposed parts of the substrate. Fig. 5 (b) shows that the silver covered by fibers remained intact, but that no trace of silver was observed on the undeposited parts, confirming that electrospun nanofibers protected the silver coating.

Morphology and height profiles of the nanofibers were characterized by AFM for the as-spun, and 7 min etched sample (see Fig. 6). The fiber diameter and thickness in nonetched regions were 715.63 ± 299.6 nm and 93.47 ± 26.96 nm, respectively (calculated based on 72 data points). On the other hand, the nanofibers in the 7 min etched regions had 518.98 ± 193.79 nm diameter and 117.36 ± 33.43 nm thickness, (calculated from 108 data points). The etching process reduced fiber diameter while protecting the nanostructures, but slightly etched away

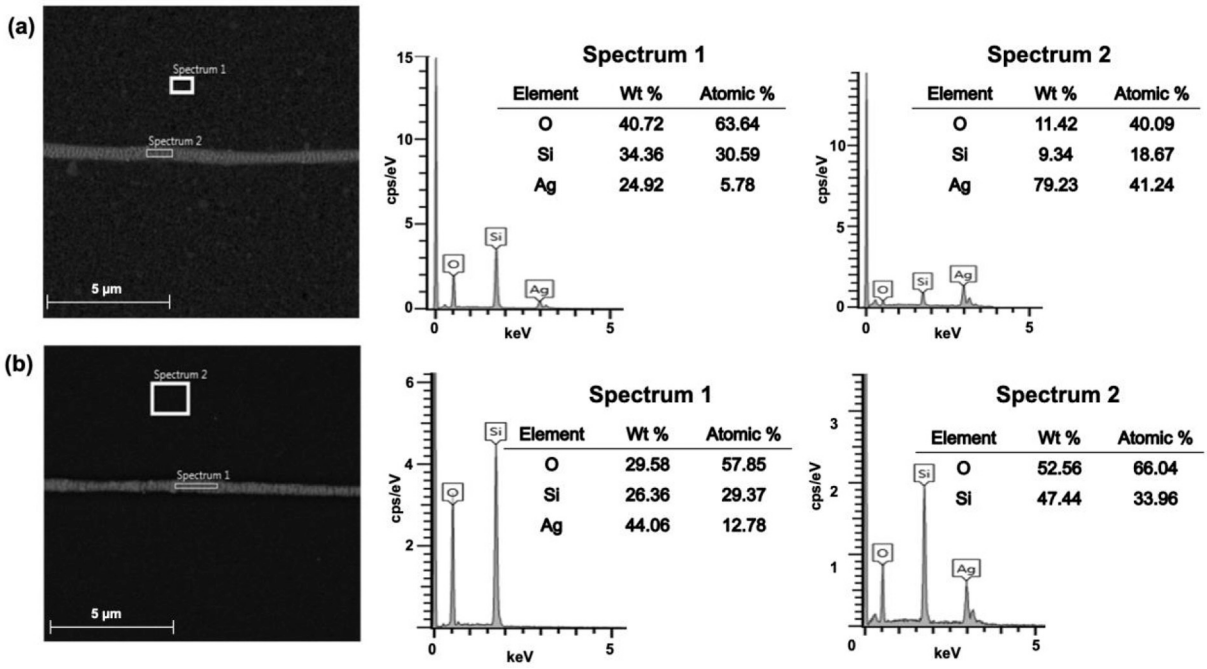

Fig. 5. EDX results of the sample fabricated at 500 V etched for a) 5 min and b) 7 min.

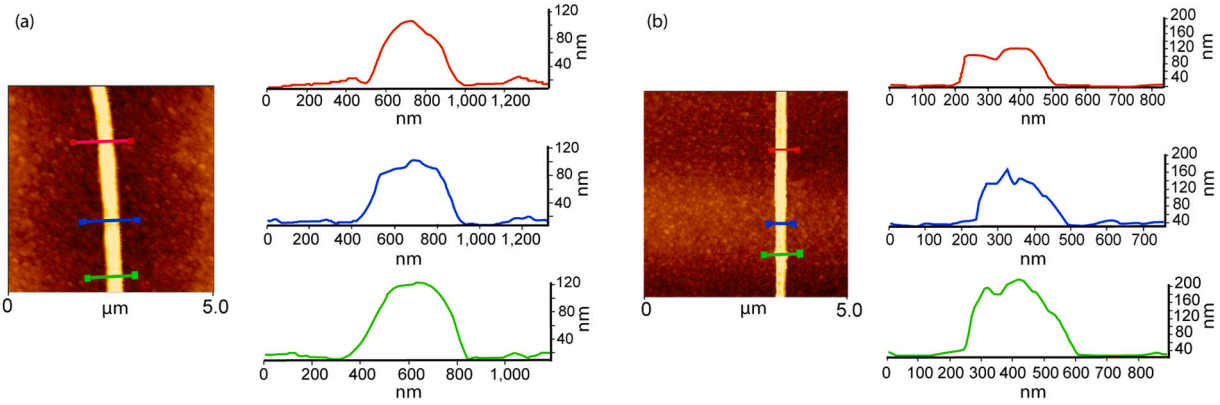

Fig. 6. AFM images and the height profiles of nanofibers electrospun at 400 V a) before the etching process b) after etching for 7 min.

the silver in the y-direction. This result suggests that longer etching times could further reduce the thickness of the silver layer, and even break the nanostructures.

The polymer on the silver nanopatterns was removed after the etching process. The width and thickness of the metallic patterns were calculated as 473.83 ± 130.39 nm and 102.04 ± 14.40 nm, respectively, from 107 data points collected by AFM. The reduction in both directions of the nanopatterns confirmed the success of the lift-off process in removing the polymer.

4. Conclusion

In summary, we presented a new strategy for the printing of Ag-based nanopatterns using electrohydrodynamic printing and reactive ion etching. This involved optimizing the process parameters for electrospinning to create precisely patterned straight nanofibers. Thus, we used two different techniques to utilize the conditions for a home-made experimental setup. In the first, the auxiliary needle mounted underneath the substrate was grounded. Although the nanofibers were successfully structured, some issues were observed in the morphology of the fibers and the patterning. In the second technique, the substrate was grounded directly, and due to the intense electric field on the substrate, the applied voltage was reduced to the range of 400–600 V. The SEM images show that straight nanofibers with a diameter of 208.7 ± 30.3 nm were successfully obtained at the voltage of 400 V. Moreover, non-uniform morphologies in the fiber structure were observed at higher voltages. The etching process was applied for different durations; under the condition of 5 min of etching, the silver regions uncoated with the fibers were not fully removed, suggesting an insufficient etching duration, while 7 min of etching of the substrates resulted in the removal of silver in the undeposited regions with protecting the silver nanostructures underneath the fibers, indicating a successful nanolithography technique. In conclusion, the procedure enabled us to use the nanofibers as a tool to obtain patterned metallic nanostructures. In future studies, the fibers will be patterned on the gold substrates, in which the interdigitated electrodes will be fabricated for miniaturized electronic devices.

Declaration of Competing Interest

The authors declare that there is no conflict of interest.

Acknowledgment

This research was supported by the Scientific and Technological Research Council of Turkey [Grant number 217M144]. We would like to thank Research and Application Center for Quantum Technologies (RACQUT). We would also like to thank Simon Mumford, Izmir University of Economics, for final proofreading of the manuscript.

References

[1] Y.L. Cheah, V. Aravindan, S. Madhavi, Synthesis and enhanced lithium storage properties of electrospun V_2O_5 nanofibers in full-cell assembly with a spinel $Li_4Ti_5O_{12}$ anode, ACS Appl. Mater. Interfaces 5 (2013) 3475–3480, https://doi.org/10.1021/am400666n.

[2] C.T. Cherian, J. Sundaramurthy, M.V. Reddy, P. Suresh Kumar, K. Mani, D. Pliszka, C.H. Sow, S. Ramakrishna, B.V.R. Chowdari, Morphologically robust $NiFe_2O_4$ nanofibers as high capacity Li-ion battery anode material, ACS Appl. Mater. Interfaces 5 (2013) 9957–9963, https://doi.org/10.1021/am401779p.

[3] K.-H. Lee, S.-S. Lee, D.B. Ahn, J. Lee, D. Byun, S.-Y. Lee, Ultrahigh areal number density solid-state on-chip microsupercapacitors via electrohydrodynamic jet printing, Sci. Adv. 6 (2020), eaaz1692, https://doi.org/10.1126/sciadv.aaz1692.

[4] Y. Ding, C. Zhu, J. Liu, Y. Duan, Z. Yi, J. Xiao, S. Wang, Y. Huang, Z. Yin, Flexible small-channel thin-film transistors by electrohydrodynamic lithography, Nanoscale. 9 (2017) 19050–19057, https://doi.org/10.1039/c7nr06075k.

[5] S.-Y. Kim, K. Kim, Y.H. Hwang, J. Park, J. Jang, Y. Nam, Y. Kang, M. Kim, H. J. Park, Z. Lee, J. Choi, Y. Kim, S. Jeong, B.S. Bae, J.U. Park, High-resolution electrohydrodynamic inkjet printing of stretchable metal oxide semiconductor transistors with high performance, Nanoscale. 8 (2016) 17113–17121, https://doi.org/10.1039/c6nr05577j.

[6] Z. Cui, Y. Han, Q. Huang, J. Dong, Y. Zhu, Electrohydrodynamic printing of silver nanowires for flexible and stretchable electronics, Nanoscale. 10 (2018) 6806–6811, https://doi.org/10.1039/c7nr09570h.

[7] M. Madadi Masouleh, J. Koohsorkhi, Moghadam R. Askari, Direct writing of individual micro/nanofiber patterns suitable for flexible electronics using MEMS-based microneedle, Microelectron. Eng. 229 (2020) 111345, https://doi.org/10.1016/j.mee.2020.111345.

[8] Q. Lei, J. He, D. Li, Electrohydrodynamic 3D printing of layer-specifically oriented, multiscale conductive scaffolds for cardiac tissue engineering, Nanoscale. (2019) 15195–15205, https://doi.org/10.1039/c9nr04989d.

[9] M. Castilho, D. Feyen, M. Flandes-Iparraguirre, G. Hochleitner, J. Groll, P.A. F. Doevendans, Melt electrospinning writing of poly-Hydroxymethylglycolide-co-ε-Caprolactone-based scaffolds for cardiac tissue engineering, Adv. Healthc Mater. 6 (2017), https://doi.org/10.1002/adhm.201700311.

[10] H. Chen, Malheiro A. de BFB, C. van Blitterswijk, C. Mota, P.A. Wieringa, L. Moroni, Direct writing electrospinning of scaffolds with multidimensional fiber architecture for hierarchical tissue engineering, ACS Appl. Mater. Interfaces 9 (2017) 38187–38200, https://doi.org/10.1021/acsami.7b07151.

[11] W. Hu, X. Ren, J. Zhang, B. Gen, S. Duan, C. Huang, Q. Mu, Y. Xi, H. Chen, High-resolution organic field-effect transistors manufactured by electrohydrodynamic inkjet printing of doped electrodes, J. Mater. Chem. (2020), https://doi.org/10.1039/D0TC02508A.

[12] J. Chang, Y. Liu, K. Heo, B.Y. Lee, S.-W. Lee, L. Lin, Direct-write complementary graphene field effect transistors and junctions via near-field electrospinning, Small. 10 (2014) 1920–1925, https://doi.org/10.1002/smll.201302965.

[13] H.-J. Kwon, X. Li, J. Hong, C.E. Park, Y.J. Jeong, H.C. Moon, S.H. Kim, Non-lithographic direct patterning of carbon nanomaterial electrodes via electrohydrodynamic-printed wettability patterns by polymer brush for fabrication of organic field-effect transistor, Appl. Surf. Sci. 515 (2020) 145989, https://doi.org/10.1016/j.apsusc.2020.145989.

[14] K.H. Lee, G.H. Kwon, S.J. Shin, J.-Y. Baek, D.K. Han, Y. Park, S.H. Lee, Hydrophilic electrospun polyurethane nanofiber matrices for hMSC culture in a microfluidic cell chip, J. Biomed. Mater. Res. A 90 (2009) 619–628, https://doi.org/10.1002/jbm.a.32059.

[15] P. Wallin, C. Zandén, B. Carlberg, N. Hellström Erkenstam, J. Liu, J. Gold, A method to integrate patterned electrospun fibers with microfluidic systems to generate complex microenvironments for cell culture applications, Biomicrofluidics. 6 (2012) 24131, https://doi.org/10.1063/1.4729747.

[16] J. Han, L. Xiong, X. Jiang, X. Yuan, Y. Zhao, D. Yang, Bio-functional electrospun nanomaterials: From topology design to biological applications, Prog. Polym. Sci. (2019) 1–28, https://doi.org/10.1016/j.progpolymsci.2019.02.006.

[17] J. Chen, T. Wu, L. Zhang, X. Feng, P. Li, F. Huang, C. Zuo, Z. Mao, Fabrication of flexible organic electronic microcircuit pattern using near-field electrohydrodynamic direct-writing method, J. Mater. Sci. Mater. Electron. (2019), https://doi.org/10.1007/s10854-019-02138-7, pp. 17863–17871.

[18] Y. Huang, N. Bu, Y. Duan, Y. Pan, H. Liu, Z. Yin, Y. Xiong, Electrohydrodynamic direct-writing, Nanoscale. 5 (2013) 12007–12017, https://doi.org/10.1039/c3nr04329k.

[19] J. Xue, T. Wu, Y. Dai, Y. Xia, Electrospinning and electrospun nanofibers: methods, materials, and applications, Chem. Rev. (2019) 5298–5415, https://doi.org/10.1021/acs.chemrev.8b00593.

[20] Y. Lee, T.-S. Kim, S.-Y. Min, W. Xu, S.-H. Jeong, H.-K. Seo, T.W. Lee, Individually position-addressable metal-nanofiber electrodes for large-area electronics, Adv. Mater. 26 (2014) 8010–8016, https://doi.org/10.1002/adma.201403559.

[21] Y. Lee, S.-Y. Min, T.-S. Kim, S.-H. Jeong, J.Y. Won, H. Kim, W. Xu, J.K. Jeong, T. W. Lee, Versatile metal Nanowiring platform for large-scale nano- and opto-electronic devices, Adv. Mater. 28 (2016) 9109–9116, https://doi.org/10.1002/adma.201602855.

[22] X. Bai, S. Liao, Y. Huang, J. Song, Z. Liu, M. Fang, C. Xu, Y. Cui, H. Wu, Continuous draw spinning of extra-Long silver submicron fibers with micrometer patterning capability, Nano Lett. 17 (2017) 1883–1891, https://doi.org/10.1021/acs.nanolett.6b05205.

[23] H. Lee, B. Seong, J. Kim, Y. Jang, D. Byun, Direct alignment and patterning of silver nanowires by electrohydrodynamic jet printing, Small. 10 (2014) 3918–3922, https://doi.org/10.1002/smll.201400936.

[24] C.-T. Pan, T.-L. Yang, Y.-C. Chen, C.-Y. Su, S.-P. Ju, K.-H. Hung, I. Wu, C.C. Hsieh, S.C. Shen, Fibers and conductive films using silver nanoparticles and nanowires by near-field electrospinning process, J. Nanomater. (2015) 1–5, https://doi.org/10.1155/2015/494052.

[25] T. Blachowicz, A. Ehrmann, Conductive electrospun nanofiber mats, Materials. 13 (2019), https://doi.org/10.3390/ma13010152.

[26] H. Yuce, H. Alaboz, Y. Demirhan, M. Ozdemir, L. Ozyuzer, G. Aygun, Investigation of electron beam lithography effects on metal–insulator transition behavior of vanadium dioxide, Phys. Scr. 92 (2017) 114007, https://doi.org/10.1088/1402-4896/aa90a3.

[27] G.S. Bisht, G. Canton, A. Mirsepassi, L. Kulinsky, S. Oh, D. Dunn-Rankin, M. J. Madou, Controlled continuous patterning of polymeric nanofibers on three-dimensional substrates using low-voltage near-field electrospinning, Nano Lett. 11 (2011) 1831–1837, https://doi.org/10.1021/nl2006164.

[28] Y. Demirhan, H. Alaboz, M.A. Nebioğlu, B. Mulla, M. Akkaya, H. Altan, C. Sabah, L. Ozyuzer, Fourcross shaped metamaterial filters fabricated from high temperature superconducting YBCO and Au thin films for terahertz waves, Supercond. Sci. Technol. 30 (2017), 074006, https://doi.org/10.1088/1361-6668/aa6fbe.

[29] W. Katzschner, A. Steckenborn, R. Löffler, N. Grote, Ion beam milling of InP with an Ar/O_2-gas mixture, Appl. Phys. Lett. (1984) 352–354, https://doi.org/10.1063/1.94725.

[30] C.H. Ding, Line and contact edge roughness meter, 2017. www.lacerm.com.

[31] D. Ye, Y. Ding, Y. Duan, J. Su, Z. Yin, Y.A. Huang, Large-scale direct-writing of aligned nanofibers for flexible electronics, Small. 14 (2018), e1703521, https://doi.org/10.1002/smll.201703521.

[32] X.-X. He, J. Zheng, G.-F. Yu, M.-H. You, M. Yu, X. Ning, Y.-Z. Long, Near-field electrospinning: progress and applications, J. Phys. Chem. C 121 (2017) 8663–8678, https://doi.org/10.1021/acs.jpcc.6b12783.

[33] T.P. Lei, X.Z. Lu, F. Yang, Fabrication of various micro/nano structures by modified near-field electrospinning, AIP Adv. (2015) 041301, https://doi.org/10.1063/1.4901879.

[34] M.M. Demir, I. Yilgor, E. Yilgor, B. Erman, Electrospinning of polyurethane fibers, Polymer. (2002) 3303–3309, https://doi.org/10.1016/s0032-3861(02)00136-2.

[35] Y. Huang, X. Wang, Y. Duan, N. Bu, Z. Yin, Controllable self-organization of colloid microarrays based on finite length effects of electrospun ribbons, Soft Matter (2012) 8302, https://doi.org/10.1039/c2sm25535a.

[36] C. Chang, K. Limkrailassiri, L. Lin, Continuous near-field electrospinning for large area deposition of orderly nanofiber patterns, Appl. Phys. Lett. (2008) 123111, https://doi.org/10.1063/1.2975834.

[37] D. Sun, C. Chang, S. Li, L. Lin, Near-field electrospinning, Nano Lett. 6 (2006) 839–842, https://doi.org/10.1021/nl0602701.